Masson,L., Tabashnik,B.E., Mazza,A., Prefontaine,G., Potvin,L., Brousseau,R., and Schwartz,J.L. (2002). Mutagenic analysis of a conserved region of domain III in the Cry1Ac toxin of Bacillus thuringiensis. Appl. Environ. Microbiol. *68*, 194-200.

Morse,R.J., Yamamoto,T., and Stroud,R.M. (2001). Structure of Cry2Aa suggests an unexpected receptor binding epitope. Structure. (Camb.) *9*, 409-417.

Parker,M.W., Buckley,J.T., Postma,J.P., Tucker,A.D., Leonard,K., Pattus,F., and Tsernoglou,D. (1994). Structure of the Aeromonas toxin proaerolysin in its water-soluble and membrane-channel states. Nature *367*, 292-295.

Parker,M.W., Pattus,F., Tucker,A.D., and Tsernoglou,D. (1989). Structure of the membrane-pore-forming fragment of colicin A. Nature *337*, 93-96.

Puntheeranurak,T., Uawithya,P., Potvin,L., Angsuthanasombat,C., and Schwartz,J.L. (2004). Ion channels formed in planar lipid bilayers by the dipteran-specific Cry4B Bacillus thuringiensis toxin and its alpha1-alpha5 fragment. Mol. Membr. Biol. *21*, 67-74.

Rajamohan,F., Alzate,O., Cotrill,J.A., Curtiss,A., and Dean,D.H. (1996). Protein engineering of Bacillus thuringiensis delta-endotoxin: mutations at domain II of CryIAb enhance receptor affinity and toxicity toward gypsy moth larvae. Proc. Natl. Acad. Sci. U. S. A *93*, 14338-14343.

Rausell,C., Munoz-Garay,C., Miranda-CassoLuengo,R., Gomez,I., Rudino-Pinera,E., Soberon,M., and Bravo,A. (2004). Tryptophan spectroscopy studies and black lipid bilayer analysis indicate that the oligomeric structure of Cry1Ab toxin from Bacillus thuringiensis is the membrane-insertion intermediate. Biochemistry *43*, 166-174.

Sangadala,S., Walters,F.S., English,L.H., and Adang,M.J. (1994). A mixture of Manduca sexta aminopeptidase and phosphatase enhances Bacillus thuringiensis insecticidal CryIA(c) toxin binding and 86Rb(+)-K+ efflux in vitro. J. Biol. Chem. *269*, 10088-10092.

Sankaranarayanan,R., Sekar,K., Banerjee,R., Sharma,V., Surolia,A., and Vijayan,M. (1996). A novel mode of carbohydrate recognition in jacalin, a Moraceae plant lectin with a beta-prism fold. Nat. Struct. Biol. *3*, 596-603.

Schnepf,E., Crickmore,N., Van Rie,J., Lereclus,D., Baum,J., Feitelson,J., Zeigler,D.R., and Dean,D.H. (1998b). Bacillus thuringiensis and its pesticidal crystal proteins. Microbiol. Mol. Biol. Rev. *62*, 775-806.

Schnepf,E., Crickmore,N., Van Rie,J., Lereclus,D., Baum,J., Feitelson,J., Zeigler,D.R., and Dean,D.H. (1998a). Bacillus thuringiensis and its pesticidal crystal proteins. Microbiol. Mol. Biol. Rev. *62*, 775-806.

Schwartz,J.L., Juteau,M., Grochulski,P., Cygler,M., Prefontaine,G., Brousseau,R., and Masson,L. (1997a). Restriction of intramolecular movements within the Cry1Aa toxin molecule of Bacillus thuringiensis through disulfide bond engineering. FEBS Lett. *410*, 397-402.

Schwartz,J.L., Potvin,L., Chen,X.J., Brousseau,R., Laprade,R., and Dean,D.H. (1997b). Single-site mutations in the conserved alternating-arginine region affect ionic channels formed by CryIAa, a Bacillus thuringiensis toxin. Appl. Environ. Microbiol. *63*, 3978-3984.

Smedley,D.P. and Ellar,D.J. (1996). Mutagenesis of three surface-exposed loops of a Bacillus thuringiensis insecticidal toxin reveals residues important for toxicity, receptor recognition and possibly membrane insertion. Microbiology *142 (Pt 7)*, 1617-1624.

Song,L., Hobaugh,M.R., Shustak,C., Cheley,S., Bayley,H., and Gouaux,J.E. (1996). Structure of staphylococcal alpha-hemolysin, a heptameric transmembrane pore. Science *274*, 1859-1866.

Tigue,N.J., Jacoby,J., and Ellar,D.J. (2001). The alpha-helix 4 residue, Asn135, is involved in the oligomerization of Cry1Ac1 and Cry1Ab5 Bacillus thuringiensis toxins. Appl. Environ. Microbiol. *67*, 5715-5720.

Uawithya,P., Tuntitippawan,T., Katzenmeier,G., Panyim,S., and Angsuthanasombat,C. (1998). Effects on larvicidal activity of single proline substitutions in alpha3 or alpha4 of the Bacillus thuringiensis Cry4B toxin. Biochem. Mol. Biol. Int. *44*, 825-832.

Vadlamudi,R.K., Weber,E., Ji,I., Ji,T.H., and Bulla,L.A., Jr. (1995). Cloning and expression of a receptor for an insecticidal toxin of Bacillus thuringiensis. J. Biol. Chem. *270*, 5490-5494.

Von Tersch,M.A., Slatin,S.L., Kulesza,C.A., and English,L.H. (1994). Membrane-permeabilizing activities of Bacillus thuringiensis coleopteran-active toxin CryIIIB2 and CryIIIB2 domain I peptide. Appl. Environ. Microbiol. *60*, 3711-3717.

Walters,F.S., Slatin,S.L., Kulesza,C.A., and English,L.H. (1993). Ion channel activity of N-terminal fragments from CryIA(c) delta-endotoxin. Biochem. Biophys. Res. Commun. *196*, 921-926.

Ward,E.S. and Ellar,D.J. (1988). Cloning and expression of two homologous genes of Bacillus thuringiensis subsp. israelensis which encode 130-kilodalton mosquitocidal proteins. J. Bacteriol. *170*, 727-735.

Ward,E.S., Ellar,D.J., and Todd,J.A. (1984). Cloning and expression in Escherichia coli of the insecticidal delta-endotoxin gene of Bacillus thuringiensis var. israelensis. FEBS Lett. *175*, 377-382.

Wolfersberger,M.G., Chen,X.J., and Dean,D.H. (1996). Site-directed mutations in the third domain of Bacillus thuringiensis delta-endotoxin CryIAa affect its ability to increase the permeability of Bombyx mori midgut brush border membrane vesicles. Appl. Environ. Microbiol. *62*, 279-282.

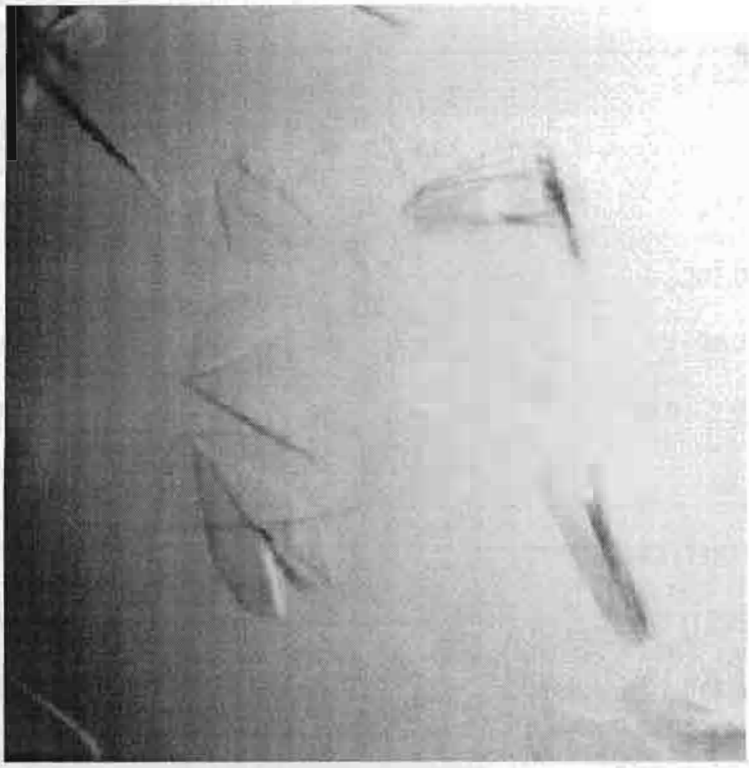

Figure 1. Crystals of Cry4Aa. Plate-shaped crystals (0.15 x 0.15 x 0.005 mm) can be seen in the crystallization drop.

Table 1.

Data collection statistics

Values in parenthesis are for the highest resolution shell (3.05-2.95 Å).

Space group	$C222_1$
Unit cell parameters (Å)	
a	91.20
b	202.07
c	98.73
Resolution range (Å)	20.0 – 2.95
Mosaicity (°)	0.5
Measured reflections	138542 (13838)
Unique reflections	19646 (1896)
Data redundancy	7.1 (7.3)
Completeness (%)	100.0 (100.0)
Average $I/\sigma(I)$	15.8 (3.7)
R_{merge}† (%)	13.4 (47.4)

† R_{merge} (%) = $(\Sigma | I_i - \langle I \rangle | / \Sigma I_i) \times 100$, where I_i is an individual intensity observation, $\langle I \rangle$ is the mean intensity for that reflection and the summation is over all reflections.

Output

Two international publications:

1 **Boonserm, P.**, Pornwiroon,W., Katzenmeier,G., Panyim,S., and Angsuthanasombat, C. (2004). Optimised expression in *Escherichia coli* and purification of the functional form of the *Bacillus thuringiensis* Cry4Aa delta-endotoxin. *Protein Expr. Purif.* **35**, 397-403.

2 **Boonserm, P.**, Angsuthanasombat, C., and Lescar J. (2004). Crystallization and preliminary crystallographic study of the functional form of the *Bacillus thuringiensis* mosquito-larvicidal Cry4Aa mutant toxin. *Acta Crystallogr. D Biol. Crystallogr.* **60**, 1315-8.

Appendix

Available online at www.sciencedirect.com
SCIENCE DIRECT®

Protein Expression and Purification 35 (2004) 397–403

Protein Expression & Purification

www.elsevier.com/locate/yprep

Optimised expression in *Escherichia coli* and purification of the functional form of the *Bacillus thuringiensis* Cry4Aa δ-endotoxin

Panadda Boonserm, Walairat Pornwiroon, Gerd Katzenmeier, Sakol Panyim, and Chanan Angsuthanasombat*

Laboratory of Molecular Biophysics, Institute of Molecular Biology and Genetics, Mahidol University, Salaya Campus, Nakornpathom 73170, Thailand

Received 10 February 2004

Abstract

Achieving high-level expression of the *Bacillus thuringiensis* Cry4Aa mosquito-larvicidal protein was demonstrated. The 130-kDa Cry4Aa protoxin was overexpressed as an inclusion body in *Escherichia coli* under the control of the *tac* promoter together with the *cry4Ba* promoter. The solubility of the toxin inclusions in carbonate buffer, pH 10.0, was markedly enhanced at a cultivation temperature of 30 °C. Elimination of the tryptic cleavage site at Arg-235 in the loop between helices 5 and 6 still retained the high-level toxicity of *E. coli* cells expressing the Cry4Aa mutant against *Aedes aegypti* larvae. Trypsin digestion of the R235Q mutant protoxin produced a protease-resistant fragment of ca. 65 kDa. A homogeneous product of the 65-kDa trypsin-treated R203Q protein was obtained after size-exclusion chromatography that would pave the way for the further crystallisation and X-ray crystallographic studies.

Keywords: *Bacillus thuringiensis*; Toxin-inclusion; Interhelical cleavage; Larvicidal activity; Mutagenesis; Size-exclusion chromatography

During sporulation, the Gram-positive spore-forming bacterium *Bacillus thuringiensis* (*Bt*) produces highly specific insecticidal crystal proteins known as δ-endotoxins [1] which are classified into two main families, Cry and Cyt δ-endotoxins, based on their deduced amino acid sequence similarity [2,3]. The Cry toxins have been shown to be toxic towards a wide variety of insect larvae in the orders Diptera, Lepidoptera, Coleoptera, and Hymenoptera [1,4]. The native *Bt* δ-endotoxins are synthesised as inactive protoxins deposited in the form of parasporal crystalline inclusions which are soluble under alkaline conditions. After ingestion by susceptible insect larvae, the toxin inclusions are exposed to the larval midgut lumen that is highly alkaline in a number of dipteran and lepidopteran insects (for reviews, see [1,4]). The liberated soluble protoxins are then processed by larval midgut proteases to yield the toxic fragments. For several Cry toxins, it has been shown that the activated toxins bind to specific receptors on the brush-border membrane of midgut epithelium. A subsequent conformational change allows the insertion of their pore-forming portion into the cell membrane to form ion-leakage pores. These leakage pores cause the target midgut cells to swell and lyse by colloid-osmotic lysis [5], resulting in extensive damage to the midgut and eventually larval death (for reviews, see [6,7]). However, the precise mechanism of toxic activity at the molecular level of the Cry toxins is still not completely elucidated.

The *Bt* Cry protoxins can be categorised into two groups based on their molecular masses. It has been shown that approximately half of the larger protoxins (120–140 kDa) is removed from the C-terminus during proteolytic activation in vitro, leaving the N-terminal half (ca. 65 kDa) as the toxic component. Activation of these protoxins is also accompanied by removal of approximately 30 residues from the N-terminus [8]. The smaller Cry protoxins (ca. 70 kDa) undergo little or no proteolysis at their C-termini, but appear to be cleaved to a greater extent than the larger Cry toxins at the N-termini where about 50 residues are removed [9,10].

---

* Corresponding author. Fax: +662-441-9906.
E-mail address: stcas@mahidol.ac.th (C. Angsuthanasombat).

46-5928/$ - see front matter © 2004 Published by Elsevier Inc.
10.1016/j.pep.2004.02.016

To date, the X-ray crystal structures of several Cry toxins, Cry1Aa [8], Cry1Ac [11,12], Cry2Aa [10], Cry3Aa [9], and Cry3Bb [13], have been elucidated, leading to a better understanding of the molecular basis of insect specificity and gut epithelial cell lysis. Although these Cry toxins show different insect specificities, they all share the similar overall tertiary structure of the three-domain organisation. The N-terminal domain I, a seven-helix bundle, has been shown to be responsible for membrane insertion and pore formation [14–17]. Domain II is composed of three anti-parallel β-sheets, each terminating in a loop at the bottom of the domain. This domain has been demonstrated to participate in receptor binding and hence is involved in insect specificity [18–21]. The C-terminal domain III is a sandwich of two anti-parallel β-sheets. The exact role of this domain is still unclear although it has been implicated in structural integrity of toxin molecules [9], membrane permeabilisation [22] or receptor recognition [23,24].

Of particular interest among bacterial insecticides, *Bt* subsp. *israelensis* (*Bti*) has been widely used in control of disease-carrying insects, i.e., mosquitoes and blackflies. This bacterium produces at least four major insecticidal crystal proteins, Cry4Aa, Cry4Ba, Cry11Aa, and Cyt1Aa, which are highly specific to such dipteran larvae [1]. Among these *Bti* toxins, Cry4Aa, and Cry4Ba (both of ca. 130 kDa) are most closely related since the C-terminal regions of their deduced amino acid sequences (ca. 465 residues) are nearly identical and their N-terminal portions share about 55% amino acid sequence similarity [25,26]. Interestingly, the Cry4Ba protein exhibits highly toxic activity towards mosquito larvae of the genera *Aedes* and *Anopheles* but has no significant activity against *Culex* larvae, whilst the Cry4Aa protein shows high toxicity against all three genera [27]. In addition, there is evidence of synergism in vivo between these two toxins against *Culex*, *Aedes*, and *Anopheles* larvae [27]. However, the precise mechanism of the synergistic interactions is still unknown. We have recently published three-dimensional models for the 65-kDa-activated Cry4Aa and Cry4Ba toxins which were constructed by homology modelling based on atomic coordinates of the Cry1Aa and Cry3Aa crystal structures [28]. It can therefore be expected that the information of the protein structures of Cry4Aa and Cry4Ba would provide considerable insight into their insecticidal function, synergistic mechanism and also facilitate the genetic improvements of toxin activity via protein engineering.

Previously, protein crystallisation and X-ray diffraction studies of the 65-kDa-activated Cry4Ba toxin were reported [29]. In the present study, the high-level production of the Cry4Aa mosquito-larvicidal protein was achieved when the *cry4Aa* gene was expressed under the control of dual promoters (P_{tac} and P_{cry4Ba}) in *E. coli*. In addition, the experimental procedures for obtaining a highly purified protease-resistant fragment representing the 65-kDa Cry4Aa functional form were demonstrated that would facilitate protein crystallisation and X-ray crystallographic analysis of this toxin.

Materials and methods

Plasmids and construction of a trypsin-site deletion mutant

The 3.65-kb DNA fragment of the full-length gene encoding the 130-kDa Cry4Aa toxin was amplified via polymerase chain reaction (PCR) from the pMU500-1 recombinant plasmid [30]. By using a PCR-based splicing by overlap extension (SOE) technique [31], the 160-bp PCR-amplified fragment of the 5′-untranslated region containing the endogenous *Bti-cryBa* promoter and the Shine–Dalgarno (SD) sequence for the *cry4Ba* gene (see Fig. 1) from the pMU388 recombinant plasmid [32] was fused in-frame with the ATG codon of the *cry4Aa* structural gene from the former PCR-amplified fragment. SOE amplification was performed using the pUC universal forward primer 5′-TTGTGAGCGGATAA CAATTTC-3′ and the pUC universal reverse primer 5′-GTTTTCCCAGTCACGACGTTGTA-3′, incorporating *Bam*HI and *Sal*I sites on the 5′ and 3′ ends of the SOE product, respectively. The fusion DNA fragment was, respectively, treated with *Bam*HI, Klenow blunting fragment and *Sal*I, and was subsequently inserted into the *Sal*I and Klenow-blunted *Eco*RI sites of the pMEx8 expression vector [33]. The resultant plasmid, pMEx-B4A (see Fig. 1), was used as a template for generating a trypsin-site deletion mutant using a pair of mutagenic oligonucleotides [forward primer, 5′-TAAAAAACAAT CAACAATTCGATTATCTAGAGCCTTTGC-3′ and reverse primer, 5′-GCAAAGGCTCTAGATAATCGA ATTGTTGATTGTTTTTTA-3′ (bold letters indicate changed nucleotides and underlined bases indicate an *Xba*I restriction site)] which were purchased from Proligo (Singapore). The trypsin site was eliminated by replacing Arg-235 with glutamine by using *Pfu* DNA polymerase via polymerase PCR-based mutagenesis (QuickChange Mutagenesis Kit, Stratagene). Selected clones with the required mutation were first identified by restriction endonuclease digestion of the plasmids and then verified by DNA sequencing, using a BigDye Terminator Cycle Sequencing Kit (Perkin–Elmer).

Toxin expression and inclusion solubilisation

Escherichia coli JM109 clones harbouring the wild-type plasmid or its mutant were grown at either 30 °C or 37 °C in a Luria–Bertani medium containing 100 µg/ml ampicillin until OD_{600} of the culture reached 0.3–0.5. Protein expression was induced with isopropyl-β-D-thiogalactopyranoside (IPTG) at a final concentration

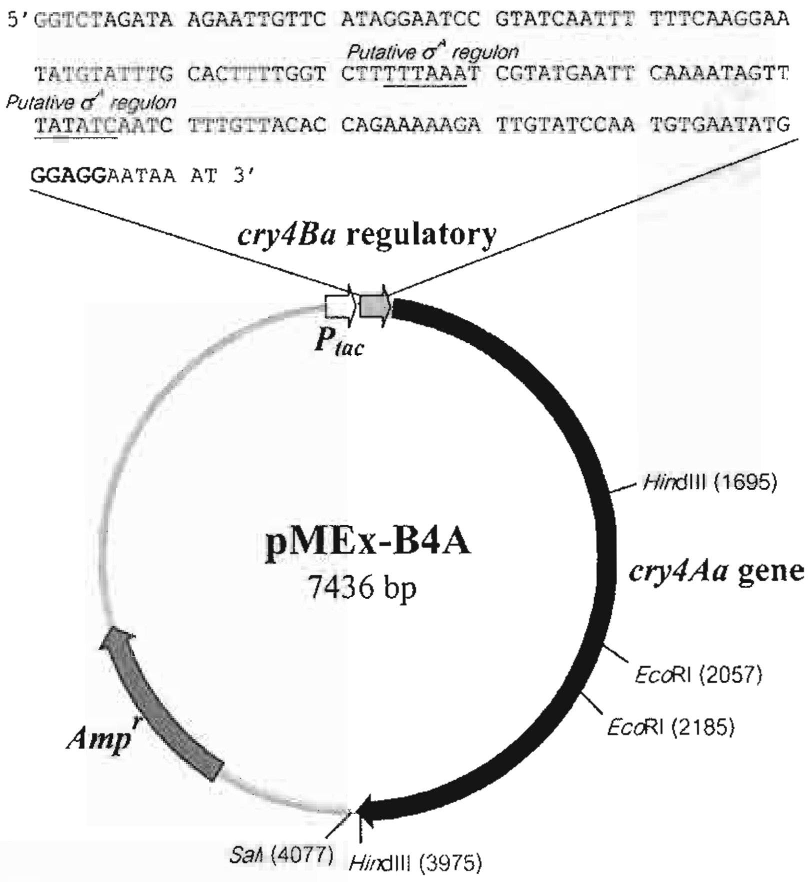

Fig. 1. Schematic map of the pMEx-B4A plasmid. This recombinant plasmid was constructed as described in the text and used for overexpressing the *cry4Aa* gene under control of the *tac* promoter (P_{tac}) and the *cry4Ba* regulatory region. The nucleotide sequences of the regulatory region (expanded view at the top of figure) are shown with the SD sequence (bold letters) and the putative σ^A regulon (underlined letters) as very similar to the *B. subtilis* σ^A regulon [37]. Amp^r indicates the ampicillin resistance gene. For clarity, not all of the restriction endonuclease sites are shown.

of 0.1 mM for 10 h and subsequently analysed by sodium dodecyl sulphate-(10% w/v) polyacrylamide gel electrophoresis (SDS–PAGE). *E. coli* cultures, which overexpress the Cry4Aa wild-type or mutant toxins as cytoplasmic inclusions, were harvested by centrifugation and resuspended in cold distilled water. Cells were then disrupted by using a French Pressure Cell at 10,000 psi. After centrifugation at 8000*g*, 4 °C for 15 min, the pellets were washed 3 times in cold distilled water and suspended by sonication. Protein concentrations of the partial-purified inclusions were determined by using a protein microassay reagent (Bio-Rad), with a bovine serum albumin fraction V (Sigma) as a standard. Inclusions (1–2 mg/ml) were solubilised by incubation at 37 °C for 1 h in 50 mM Na_2CO_3, pH 10.0. Solubilised protoxins were then separated from insoluble materials by centrifugation at 12,000*g* for 15 min.

Proteolytic activation and active-toxin purification

The 130-kDa solubilised Cry4Aa protoxins were mixed with trypsin (L-1-tosylamide-2-phenylethyl chloromethyl ketone treated, Sigma) at an enzyme:protoxin ratio of 1:10 (w/w) and incubated at 37 °C for 16 h. The proteolytic reaction was then stopped by adding 1 mM tosyl-lysine chloromethyl ketone (TLCK). After being examined by SDS–PAGE in comparison with the solubilised protoxin fraction, the trypsin-activated fraction was concentrated by ultrafiltration at 4 °C using a Centriprep column (30-kDa cutoff, Amicon) and further purified by a size-exclusion FPLC system (Superdex 200, Amersham–Pharmacia Biotech) with a linear gradient of 50 mM Na_2CO_3, pH 10.0, at a flow rate of 0.4 ml/min. Eluted fractions across the 65-kDa protein peak were pooled and concentrated to 3–5 mg/ml by ultrafiltration as described above.

Larvicidal activity assays

Bioassays for mosquito-larvicidal activity were performed as previously described [34], using 2-day-old *Aedes aegypti* larvae (hatched from eggs supplied by the mosquito-rearing facility of the Institute of Molecular Biology and Genetics, Mahidol University, Thailand). Both rearing and bioassays were carried out at room temperature (25 °C). The assays were done in 1 ml *E. coli* suspension (10^8 cells suspended in distilled water) in a 48-well titration plate (11.3-mm well diameter, Costar, USA), with 10 larvae per well and a total of 100 larvae for each type of *E. coli* sample. *E. coli* cells containing the pMEx8 vector were used as a negative control. Mortality was recorded after 24-h incubation period.

Results and discussion

Previously, we have demonstrated that the high-level expression of the cloned *cry4Ba* gene in *E. coli* was driven by both the endogenous *Bti* promoter (located within the 160-bp 5′-upstream region) and the *lacZ* promoter of the pUC12 vector, yielding a cytoplasmic inclusion of the 130-kDa Cry4Ba protoxin [32]. On the other hand, the closely related *Bti* toxin, i.e., the 130-kDa Cry4Aa mosquito-larvicidal protein, was produced at lower amounts in a soluble form, despite the fact that its expression is also under the control of the *lacZ* promoter in the same plasmid vector and organism [30]. In this study, an initial attempt was made to construct a fusion DNA fragment in which the 160-bp *cry4Ba* regulatory fragment containing both the SD sequence (GGAGG) and the putative *Bti*-σ^A regulon (see Fig. 1) was fused in-frame with the translation start codon of the *cry4Aa* structural gene segment. The *cry4Ba* regulatory region was found to significantly increase the expression of the 130-kDa Cry4Aa protein in *E. coli* cells regardless of whether it is expressed in an expression (pUC12) or non-expression (pUN121) vector (data not shown). Despite higher protein production, the expressed Cry4Aa protoxin under regulation of the *lacZ* promoter together with the *cry4Ba* regulatory element was retained mainly in the soluble fraction. To improve the level of Cry4Aa expression that would lead to a toxin-inclusion formation, the fusion DNA fragment which contains the *cry4Ba* regulatory region and the *cry4Aa* structural gene was therefore subcloned into the pMEx8 vector under control of the stronger promoter (P_{tac}). It was found that *E. coli* cells harbouring the resultant recombinant plasmid (pMEx-B4A) were able to express the 130-kDa Cry4Aa toxin almost exclusively as a sedimentable inclusion body upon IPTG induction (Fig. 2, lanes 1 and 3). This indicates that the strong inducible *tac* promoter together with the *cry4Ba* regulatory element could confer the high-level expression of the Cry4Aa protein, leading to the formation of a toxin inclusion.

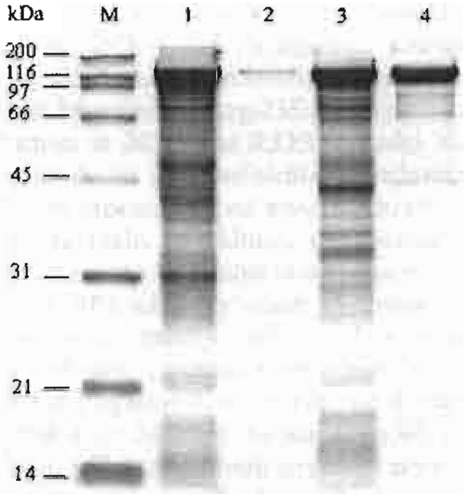

Fig. 2. Coomassie-stained SDS–PAGE (12% gel) showing protein solubility of the partially purified Cry4Aa toxin inclusions extracted from *E. coli* cultures grown at 37 °C (lanes 1 and 2) and at 30 °C (lanes 3 and 4). Solubilisation was carried out in carbonate buffer, pH 10.0, for 1 h. Lanes 1 and 3, the total inclusion fractions; lanes 2 and 4, an equivalent amount of the supernatant containing the 130-kDa solubilised protoxins after centrifugation. M indicates molecular mass standards.

Dissimilar to the Cry4Ba protoxin inclusion, the Cry4Aa inclusion isolated from the *E. coli* cultures that were grown at 37 °C was found to be scarcely solubilised in the carbonate buffer, pH 10.0 (Fig. 2, lane 2). At this stage, the reason for this difference in solubility in vitro between these two closely toxin inclusions is not clear and no definitive correlation has been currently established between the amino acid sequence of a protein and its propensity to form an insoluble aggregate in vivo. Nevertheless, it was interestingly found that the solubility of the Cry4Aa inclusion was enhanced by approximately 60–70% when cultivation was at 30 °C, albeit a lower-level expression (Fig. 2, lane 4). This implies that decreasing the growth temperature would reduce the rate of protein synthesis which should disfavour misfolding of the Cry4Aa toxin. Protein misfolding can be attributed to the intracellular concentration of aggregation-prone intermediates that would consequently affect inclusion body formation as demonstrated by a drastically perturbed dissolvability of the Cry4Aa toxin inclusion produced from the cultivation at 37 °C.

As previously demonstrated, both the 130-kDa Cry4Aa and Cry4Ba toxins were cleaved by trypsin into ca. 20- and 47-kDa fragments, in addition to the removal of the C-terminal half of the protoxins [27,35]. These two trypsin-resistant fragments were produced by the cleavage at Arg-235 and Arg-203 located in the exposed loop connecting helices 5 and 6 within the pore-forming domain of Cry4Aa and Cry4Ba, respectively. These two fragments were also found associated to each other under physiological conditions [27,35]. Additionally, alanine substitution of Arg-203 resulting in blocking the tryptic cleavage site of the Cry4Ba toxin was previously shown

Table 1
Larvicidal activity of *E. coli* cells expressing Cry4Aa or its mutant

E. coli clones containing plasmids	Percent mortality ± SEM[a]
pMEx8 (negative control)	1.7 ± 0.3
pMEx-B4A (wild type)	91.3 ± 0.3
R235Q	89.7 ± 1.2

[a] The data represent means ± SEM (standard error of the mean) based on three independent experiments.

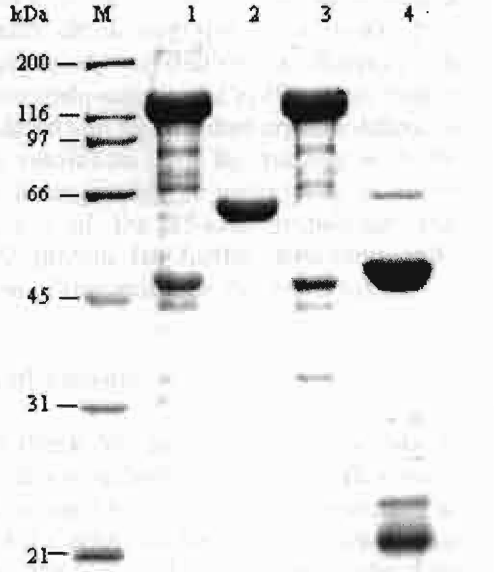

Fig. 3. Coomassie-stained SDS–PAGE (12% gel) showing proteolytic processing of Cry4Aa and its mutant (R235Q). M, molecular mass standards; lanes 1 and 2, the 130-kDa protoxin of R235Q mutant and its 65-kDa major trypsin-activated product, respectively; and lanes 3 and 4, the 130-kDa protoxin of wild-type Cry4Aa and its trypsin-activated products, respectively.

to increase the larvicidal activity at least twofold [35,36]. Here, the same PCR-based mutagenesis strategy was employed to eliminate the interhelical cleavage of the Cry4Aa toxin by mutating Arg-235 to glutamine. Upon IPTG induction at 30 °C, the R235Q mutant was predominantly produced as a sedimentable inclusion body and the protein expression level was comparable to that of the wild-type toxin. In addition, the purified mutant inclusion was found to be soluble in carbonate buffer, pH 10.0, giving ca. 70% solubility which resembles the wild-type inclusion under similar conditions (data not shown).

When *E. coli* cells expressing the mutant toxin were tested for toxicity against *A. aegypti* larvae, the mortality data recorded after 24-h incubation revealed that the R235Q mutant still retained high larvicidal activity similar to that of the wild type (Table 1). This indicated that the trypsin-site mutation had no adverse effect on the Cry4Aa toxin toxicity. The 130-kDa solubilised mutant protoxin was also assessed for its proteolytic stability by digestion with trypsin and found to produce a major trypsin-resistant fragment of 65 kDa (Fig. 3). Upon purification using size-exclusion FPLC, the 65-kDa fragment was eluted from the column in the peak corresponding to the eluted fractions of the 67-kDa BSA protein marker, indicating that it exists in a monomeric form. As assessed by SDS–PAGE (see Fig. 4), high purity of the

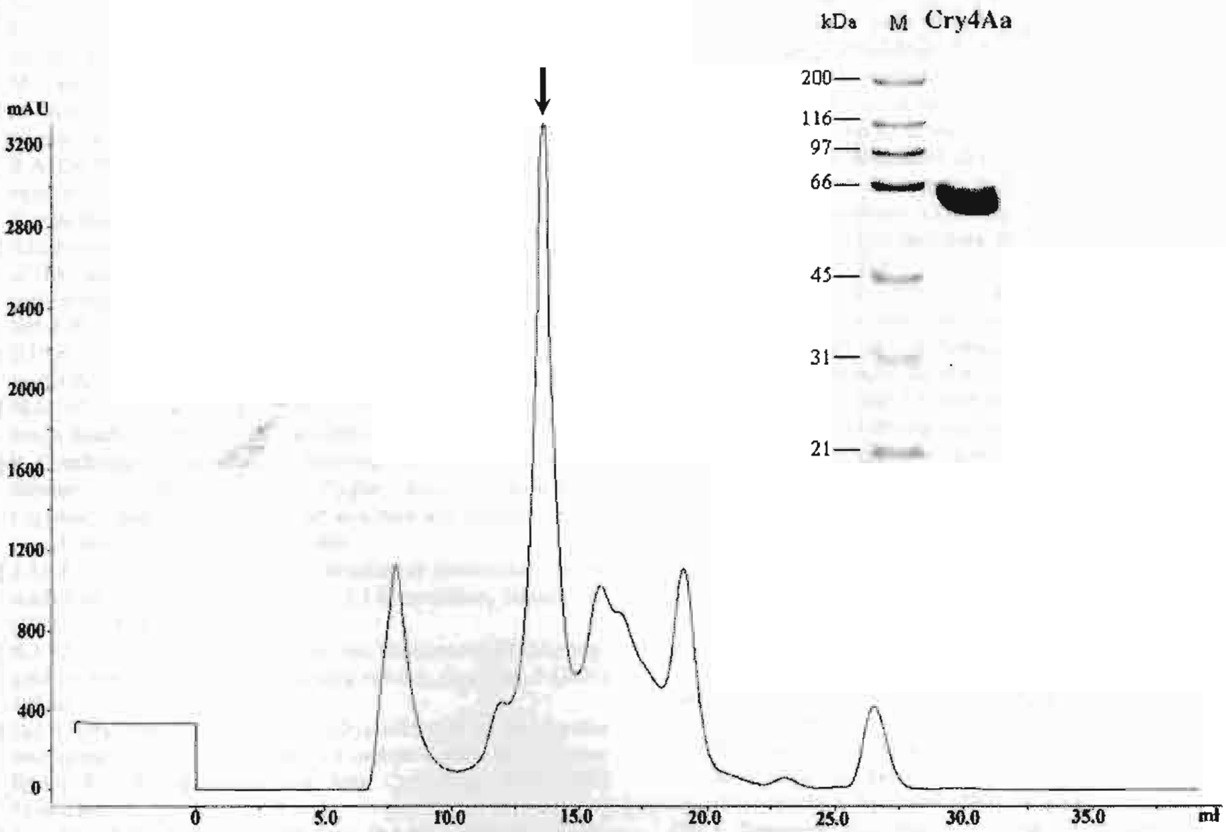

Fig. 4. Protein purification of the 65-kDa trypsin-activated Cry4Aa mutant (R235Q) by size-exclusion chromatography. Elution profile from Superdex 200 (Pharmacia) showing absorbance at 280 nm (mAU) and elution volume (ml). Inset, gel photograph for SDS–PAGE analysis of a selected peak fraction (arrowed) containing the 65-kDa Cry4Aa fragment. M represents molecular mass standards.

65-kDa Cry4Aa-R235Q protein was obtained after size-exclusion chromatography that would be favourable for subsequent crystallisation. Recently, the 68-kDa chymotrypsin-activated Cry4Ba toxin was successfully crystallised and well-formed crystals diffracted X-rays to 1.75 Å resolution [29]. By analogy with the previous study, attempts will be undertaken to promote crystal formation of the 65-kDa trypsin-activated Cry4Aa R235Q protein for further structural and functional analysis of this mosquito-larvicidal toxin.

Acknowledgments

We thank Ms. Somsri Sakdee and Ms. Chaweewan Shimwai for technical assistance. This work was supported in part by the Thailand Research Fund and the National Center for Genetic Engineering and Biotechnology, the National Science and Technology Development Agency of Thailand.

References

[1] E. Schnepf, N. Crickmore, J. Van Rie, D. Lereclus, J. Baum, J. Feitelson, D.R. Zeigler, D.H. Dean, *Bacillus thuringiensis* and its pesticidal crystal proteins, Microbiol. Mol. Biol. Rev. 62 (1998) 775–806.

[2] N. Crickmore, D.R. Zeigler, J. Feitelson, E. Schnepf, J. van Rie, D. Lereclus, J. Baum, D.H. Dean, Revision of the nomenclature for the *Bacillus thuringiensis* pesticidal crystal proteins, Microbiol. Mol. Biol. Rev. 62 (1998) 807–813.

[3] H. Höfte, H.R. Whiteley, Insecticidal crystal proteins of *Bacillus thuringiensis*, Microbiol. Rev. 53 (1989) 242–255.

[4] R.A. De Maagd, A. Bravo, N. Crickmore, How *Bacillus thuringiensis* has evolved specific toxins to colonize the insect world, Trends Genet. 4 (2001) 193–199.

[5] B.H. Knowles, D.J. Ellar, Colloid-osmotic lysis is a general feature of the mechanism of action of *Bacillus thuringiensis* δ-endotoxin with different insect specificity, Biochim. Biophys. Acta 924 (1987) 509–518.

[6] B.H. Knowles, Mechanism of action of *Bacillus thuringiensis* insecticidal delta-endotoxins, Adv. Insect Physiol. 24 (1994) 275–308.

[7] M.E. Whalon, B.A. Wingerd, Bt: mode of action and use, Arch. Insect Biochem. Physiol. 54 (2003) 200–211.

[8] P. Grochulski, L. Masson, S. Borisova, M. Pusztai-Carey, J.L. Schwartz, R. Brousseau, M. Cygler, *Bacillus thuringiensis* CryIA(a) insecticidal toxin crystal structure and channel formation, J. Mol. Biol. 254 (1995) 447–464.

[9] J. Li, J. Carroll, D.J. Ellar, Crystal structure of insecticidal δ-endotoxin from *Bacillus thuringiensis* at 2.5 Å resolution, Nature 353 (1991) 815–821.

[10] R.J. Morse, T. Yamamoto, R.M. Stroud, Structure of Cry2Aa suggests an unexpected receptor binding epitope, Structure 9 (2001) 409–417.

[11] D.J. Derbyshire, D.J. Ellar, J. Li, Crystallization of the *Bacillus thuringiensis* toxin Cry1Ac and its complex with the receptor ligand *N*-acetyl-D-galactosamine, Acta Crystallogr. D57 (2001) 1938–1944.

[12] J. Li, D.J. Derbyshire, B. Promdonkoy, D.J. Ellar, Structure implications for the transformation of the *Bacillus thuringiensis* δ-endotoxins from water-soluble to membrane-inserted forms, Biochem. Soc. Trans. 29 (2001) 571–577.

[13] N. Galitsky, V. Cody, A. Wojtczak, D. Ghosh, J.R. Luft, W. Pangborn, L. English, Structure of the insecticidal bacterial δ-endotoxin Cry3Bb1 of *Bacillus thuringiensis*, Acta Crystallogr. D57 (2001) 1101–1109.

[14] F.S. Walters, S.L. Slatin, C.A. Kulesza, L.H. English, Ion channel activity of N-terminal fragments from CryIA(c) delta-endotoxin, Biochem. Biophys. Res. Commun. 196 (1993) 921–926.

[15] M.A. Von Tersch, S.L. Slatin, C.A. Kulesza, L.H. English, Membrane-permeabilizing activities of *Bacillus thuringiensis* coleopteran-active toxin CryIIIB2 and CryIIIB2 domain I peptide, Appl. Environ. Microbiol. 60 (1994) 3711–3717.

[16] T. Puntheeranurak, S. Leetachewa, G. Katzenmeier, C. Krittanai, S. Panyim, C. Angsuthanasombat, Expression and biochemical characterization of the *Bacillus thuringiensis* Cry4B α1-α5 pore-forming fragment, J. Biochem. Mol. Biol. 34 (2001) 293–298.

[17] T. Puntheranurak, P. Uawithya, L. Potvin, C. Angsuthanasombat, J.-L. Schwartz, Ion channels formed in planar lipid bilayers by the dipteran-specific Cry4B *Bacillus thuringiensis* and its α1–α5 fragment, Mol. Membr. Biol. 21 (2003) 67–74.

[18] D.P. Smedley, D.J. Ellar, Mutagenesis of three surface-exposed loops of a *Bacillus thuringiensis* insecticidal toxin reveals residues important for toxicity, receptor recognition and possibly membrane insertion, Microbiology 142 (1996) 1617–1624.

[19] F. Rajamohan, S.R. Hussain, J.A. Cotrill, F. Gould, D.H. Dean, Mutations at domain II, loop 3, of *Bacillus thuringiensis* CryIAa and CryIAb delta-endotoxins suggest loop 3 is involved in initial binding to lepidopteran midguts, J. Biol. Chem. 271 (1996) 25220–25226.

[20] V. Ballester, F. Granero, B.E. Tabashnik, T. Malvar, J. Ferre, Integrative model for binding of *Bacillus thuringiensis* toxins in susceptible and resistant larvae of the diamondback moth (*Plutella xylostella*), Appl. Environ. Microbiol. 65 (1999) 2503–2507.

[21] J.-L. Jurat-Fuentes, M.J. Adang, Importance of Cry1 delta-endotoxin domain II loops for binding specificity in *Heliothis virescens* (L.), Appl. Environ. Microbiol. 67 (2001) 323–329.

[22] L. Masson, B.E. Tabashnik, A. Mazza, G. Prefontaine, L. Potvin, R. Brousseau, J.-L. Schwartz, Mutagenic analysis of a conserved region of domain III in the Cry1Ac toxin of *Bacillus thuringiensis*, Appl. Environ. Microbiol. 68 (2002) 194–200.

[23] M.K. Lee, B.A. Young, D.H. Dean, Domain III exchanges of *Bacillus thuringiensis* CryIA toxins affect binding to different gypsy moth midgut receptors, Biochem. Biophys. Res. Commun. 216 (1995) 306–312.

[24] S.L. Burton, D.J. Ellar, J. Li, D.J. Derbyshire, *N*-acetylgalactosamine on the putative insect receptor aminopeptidase N is recognized by a site on the domain III lectin-like fold of a *Bacillus thuringiensis* insecticidal toxin, J. Mol. Biol. 287 (1999) 1101–1122.

[25] S. Ward, D.J. Ellar, Cloning and expression of two homologous genes of *Bacillus thuringiensis* subsp. *israelensis* which encode 130-kilodalton mosquitocidal proteins, J. Bacteriol. 170 (1998) 727–735.

[26] W. Chungjatupornchai, H. Hofte, J. Seurinck, C. Angsuthanasombat, M. Vaeck, Common features of *Bacillus thuringiensis* toxins specific for Diptera and Lepidoptera, Eur. J. Biochem. 173 (1988) 9–16.

[27] C. Angsuthanasombat, N. Crickmore, D.J. Ellar, Comparison of *Bacillus thuringiensis* subsp. *israelensis* CryIVA and CryIVB cloned toxins reveals synergism in vivo, FEMS Microbiol. Lett. 94 (1992) 63–67.

[28] C. Angsuthanasombat, P. Uawithya, S. Leetachewa, W. Pornwiroon, P. Ounjai, T. Kerdcharoen, G. Katzenmeier, S. Panyim, *Bacillus thuringiensis* Cry4A and Cry4B mosquito-larvicidal proteins: homology-based 3D model and implications for toxin activity, J. Biochem. Mol. Biol. (2004), in press.

[29] P. Boonserm, D.J. Ellar, J. Li, Crystallisation and preliminary X-ray diffraction studies of a mosquito-larvicidal toxin from *Bacillus thuringiensis* subsp. *israelensis*, Acta Crystallogr. D 59 (2003) 591–594.

S. Panyim, C. Angsuthanasombat, M. Pao-Intara, P. Laxananil, W. Leelamanit, Genetic engineering of *Bacillus thuringiensis* var. *israelensis* genes for biocontrol of mosquito vectors of diseases in tropical regions, Isr. J. Entomol. 23 (1989) 219–225.

M. Horton, In vitro recombination and mutagenesis of DNA: SOEing together tailor-made genes, in: B.A. White (Ed.), Methods in Molecular Biology, Humana Press, Totowa, 1993, pp. 251–261.

[32] C. Angsuthanasombat, W. Chungjatupornchai, S. Kertbundit, P. Luxananil, C. Settasatian, P. Wilairat, S. Panyim, Cloning and expression of 130-kd mosquito-larvicidal delta-endotoxin gene of *Bacillus thuringiensis* var. *israelensis* in *Escherichia coli*, Mol. Gen. Genet. 208 (1987) 384–389.

33] V. Buttcher, A. Ruhlmann, F. Cramer, Improved single stranded-DNA producing expression vectors for protein manipulation in *Escherichia coli*, Nucleic Acids Res. 18 (1990) 1075–1078.

[34] I. Sramala, P. Uawithya, U. Chanama, S. Leetachewa, C. Krittanai, G. Katzenmeier, S. Panyim, C. Angsuthanasombat, Single proline substitutions of selected helices of the *Bacillus thuringiensis* Cry4B toxin affect inclusion solubility and larvicidal activity, J. Biochem. Mol. Biol. Biophys. 4 (2000) 187–193.

[35] C. Angsuthanasombat, N. Crickmore, D.J. Ellar, Effects on toxicity of eliminating a cleavage site in a predicted interhelical loop in *Bacillus thuringiensis* CryIVB δ-endotoxin, FEMS Microbiol. Lett. 111 (1993) 255–262.

[36] M.A.F. Adullah, O. Alzate, M. Mohammad, R.J. McNall, M.J. Adang, D.H. Dean, Introduction of Culex toxicity into *Bacillus thuringiensis* Cry4Ba by protein engineering, Appl. Environ. Microbiol. 69 (2003) 5343–5353.

[37] C.A. Gross, M. Lonetto, R. Losick, Bacterial sigma factors, in: S.L. McKnight, K.R. Yamamoto (Eds.), Transcriptional Regulation, Cold Spring Harbor Laboratory Press, New York, 1992, pp. 129–176.

Acta Crystallographica Section D
Biological Crystallography
ISSN 0907-4449

Crystallization and preliminary crystallographic study of the functional form of the *Bacillus thuringiensis* mosquito-larvicidal Cry4Aa mutant toxin

Panadda Boonserm,[a]* Chanan Angsuthanasombat[a] and Julien Lescar[b]

[a]Institute of Molecular Biology and Genetics, Mahidol University, Salaya Campus, Nakornpathom 73170, Thailand, and [b]School of Biological Sciences, Nanyang Technological University, 60 Nanyang Drive, Singapore 637551, Singapore

Correspondence e-mail: mbpbs@mahidol.ac.th

Received 5 March 2004
Accepted 9 May 2004

The 65 kDa functional form of the mosquito-larvicidal Cry4Aa-R235Q mutant toxin has been crystallized. The crystals belong to space group $C222_1$, with unit-cell parameters $a = 91.2$, $b = 202.1$, $c = 98.7$ Å, and contain one molecule per asymmetric unit. The crystals diffract to $\sim$2.9 Å using synchrotron radiation and a complete native data set has been collected. The structure has been solved using a molecular-replacement method with the Cry4Ba toxin protein as a search model.

1. Introduction

During sporulation, the Gram-positive bacterium *Bacillus thurigiensis* (Bt) expresses insecticidal crystal proteins known as δ-endotoxins, which are grouped into two major families: Cry and Cyt δ-endotoxins (Crickmore *et al.*, 1998). Depending on the bacterial isolates, these crystal proteins are toxic towards a variety of insect larvae of the orders Lepidoptera (moths and butterflies), Diptera (mosquitoes and blackflies), Coleoptera (beetles and weevils) and Hymenoptera (wasps and bees) (Schnepf *et al.*, 1998). Bt δ-endotoxins are synthesized as inactive protoxins that are processed by larval midgut proteases into their active form. The activated toxin then binds to a specific receptor on the midgut epithelial cells and inserts into the cell membrane, creating ion-leakage pores that cause cell swelling and eventually cell death by colloid osmotic lysis (Knowles, 1994).

Several three-dimensional crystal structures of Cry δ-endotoxins, namely Cry3Aa (Li *et al.*, 1991), Cry1Aa (Grochulski *et al.*, 1995), Cry1Ac (Li *et al.*, 2001), Cry3Bb (Galitsky *et al.*, 2001) and Cry2Aa (Morse *et al.*, 2001), have been elucidated. Recently, the crystallization of the 68 kDa active fragment of the dipteran-specific Cry4Ba was reported (Boonserm *et al.*, 2003). Active Cry toxins (60–70 kDa) are composed of three globular domains: a helix bundle (domain I), a domain containing anti-parallel β-strands with a Greek-key topology (domain II) and a β-sandwich with jelly-roll topology (domain III). Since the N-terminal domain I contains amphipathic α-helices surrounding a central hydrophobic α-helix that is long enough to span a lipid bilayer, it was proposed that after a large conformational change this domain could insert into the membrane of the host cell to form a pore (Li *et al.*, 1991; Grochulski *et al.*, 1995). This prediction was subsequently validated by expressing isolated domain I fragments or synthetic helices that were shown to penetrate the membrane and form ion-permeable pores (Walters *et al.*, 1993; Von Tersch *et al.*, 1994; Gazit *et al.*, 1998; Puntheeranurak *et al.*, 2004). Domain II plays a role in binding to receptors at the surface of the insect midgut. Site-directed mutagenesis targeting three exposed loops at the apex of domain II identified the residues that were involved in receptor binding of several insect species (Smedley & Ellar, 1996; Rajamohan *et al.*, 1996; Jurat-Fuentes & Adang, 2001), suggesting a role of these loop regions as the primary determinant of insect specificity. The C-terminal domain III could be involved in preserving the structural integrity of toxin molecules (Li *et al.*, 1991), in determining specificity (Lee *et al.*, 1995; Burton *et al.*, 1999) and in the regulation of ion-channel activity (Chen *et al.*, 1993; Wolfersberger *et al.*, 1996; Schwartz *et al.*, 1997).

Bacillus thuringiensis subsp. *israelensis* (Bti) is highly toxic towards the larvae of *Aedes*, *Culex* and *Anopheles*, which are vectors of dengue fever, filariasis and malaria, respectively (Roberts, 2002). This bacterium produces four major insecticidal proteins: Cry4Aa, Cry4Ba, Cry11Aa and Cyt1Aa (Schnepf *et al.*, 1998). Of these, Cry4Aa and Cry4Ba are most closely related, with about 55% sequence similarity. Although both proteins are toxic towards mosquito larvae, their level of toxicity towards the various mosquito species varies. In the absence of an experimental three-dimensional structure, putative loop residues from Cry4Aa (specific against *Culex* and to a lesser extent *Aedes* larvae) were exchanged with the corresponding residues from Cry4Ba (specific against *Aedes* and *Anopheles* larvae). Exchanging loop 3 of domain II resulted in a significant increase of toxicity towards *Culex*, with no significant decrease towards *Aedes* larvae (Abdullah *et al.*, 2003). It was reported that both Cry4Aa and Cry4Ba protoxins were cleaved by trypsin into fragments of about 20 and 45 kDa, in addition to the removal of the C-terminal half of the toxins (Yamagiwa *et al.*, 1999; Angsuthanasombat *et al.*, 1993). These fragments were produced by trypsin cleavage at Arg235 and Arg203 of Cry4Aa and Cry4Ba, respectively. As previously reported, alanine substitution of Arg203, resulting in blocking the tryptic cleavage site of Cry4Ba, was shown to increase larvicidal activity (Angsuthanasombat *et al.*, 1993; Abdullah *et al.*, 2003). Additionally, elimination of the tryptic cleavage site at Arg235 by glutamine substitution (R235Q) led to retention of the high-level toxicity of the Cry4Aa mutant against *Aedes aegypti* larvae, indicating that the trypsin-site mutation had no adverse effect on the Cry4Aa toxin toxicity (Boonserm *et al.*, 2004).

Given the widespread emergence of resistance towards conventional pest-control agents, bacterial Cry proteins are of great interest for the development of new specific bio-insecticides. Thus, the availability of experimentally determined three-dimensional structures will be of great use in order to help in the the design of rationally modified toxins with altered specificity and improved potency. Here, we report the purification, crystallization, data collection and structure determination of the Cry4Aa-R235Q active mutant from Bti.

2. Materials and methods

2.1. Protein expression and solubilization

Escherichia coli JM109 cells harbouring a single amino-acid Cry4Aa mutant (see §3.1 below) were grown at 303 K in Luria–Bertani medium containing 100 µg ml^{-1} ampicillin until the OD$_{600}$ of the culture reached 0.3–0.5. Protein expression was induced with isopropyl-β-D-thiogalactopyranoside (IPTG) at a final concentration of 0.1 m*M* for 10 h and the culture was analysed by sodium dodecyl sulfate–10%(*w*/*v*) polyacrylamide gel electrophoresis (SDS–PAGE). *E. coli* cultures overexpressing the Cry4Aa single amino-acid mutant toxin as cytoplasmic inclusions were harvested by centrifugation and resuspended in cold distilled water. The cell suspension was then disrupted using a French pressure cell at 69 MPa. After centrifugation at 8000*g* at 277 K for 15 min, the pellets were washed three times in cold distilled water and resuspended by sonication. The protein concentrations of the partially purified inclusions were determined using a protein microassay reagent (Bio-Rad), with bovine serum albumin fraction V (Sigma) as a standard. Inclusions at a concentration of about 2 mg ml^{-1} were solubilized by incubation at 310 K for 1 h in 50 m*M* Na_2CO_3 pH 10.0. Solubilized protoxins were then separated from insoluble materials by centrifugation at 12 000*g* for 15 min.

2.2. Proteolytic activation and active-toxin purification

The 130 kDa solubilized Cry4Aa protoxins were mixed with trypsin (L-1-tosylamide-2-phenylethyl chloromethyl ketone-treated, Sigma) at an enzyme:protoxin ratio of 1:10(*w*/*w*) and incubated at 310 K for 16 h. Proteolysis was stopped by adding 1 m*M* tosyl-lysine chloromethyl ketone (TLCK). After analysis by SDS–PAGE, the trypsin-activated fraction was concentrated at 277 K using a Centriprep ultrafiltration device with a 30 kDa molecular-weight cutoff (Amicon). The protein was further purified by size-exclusion chromatography on an FPLC system (Superdex 200, Amersham Pharmacia Biotech) in 50 m*M* Na_2CO_3 pH 10.0 at a flow rate of 0.4 ml min^{-1}. Under these conditions, the 65 kDa Cry4Aa toxin elutes as a monomer, as shown by using BSA (67 kDa) as a marker. Eluted fractions containing the proteins were pooled and concentrated to 3–5 mg ml^{-1} by ultrafiltration as described above.

2.3. Crystallization and data collection

Crystals were grown using the hanging-drop vapour-diffusion technique. 5 µl precipitant solution was mixed with an equal volume of purified Cry4Aa at a concentration of 3–5 mg ml^{-1}. The drop was equilibrated against a reservoir containing 1 ml of the precipitant solution at 296 K. The purified protein in 50 m*M* Na_2CO_3 pH 10.0 was first mixed with solutions of 0.1 *M* Tris–acetate at pH values of between 7 and 9. Several precipitants, including salts, various molecular-weight polyethylene glycols (PEG), glycerol and 2-methyl-2,4-pentanediol (MPD), were tested. However, crystals only appeared in the conditions containing salts. Clusters of needle-like crystals were found in 0.1 *M* Tris–acetate pH 7.0 and 0.3–0.4 *M* Li_2SO_4. Microcrystals appeared after two weeks in 0.1 *M* Tris–acetate pH 7.0 and 0.2–0.3 *M* LiCl. However, in both cases crystals were too small and too poorly ordered for X-ray diffraction studies. Clusters of thin plate-shaped crystals were successively obtained using a protein concentration greater than 5 mg ml^{-1} in precipitant solution containing 0.1 *M* Tris–acetate pH 7.0 and 0.2–0.3 *M* KH_2PO_4. This condition was optimized by lowering the protein concentration to 3–5 mg ml^{-1}.

For data collection, crystals were soaked briefly in a cryoprotectant solution containing 20% 2-methyl-2,4-pentanediol (MPD), 10% polyethylene glycol (PEG) 400 and 0.1 *M* Tris–acetate and 0.3 *M* KH_2PO_4pH 7.0 before being mounted in a cryoloop and cooled to 100 K in a nitrogen-gas stream (Oxford Cryosystems). Measurements were made at an X-ray wavelength of 0.976 Å at ESRF beamline ID29 with an attenuated beam of dimensions 0.1 × 0.1 mm. Diffraction intensities were recorded on an ADSC Quantum IV CCD detector. The crystal-to-detector distance was set to 250 mm and the oscillation angle for each of the 180 images recorded was 1°. Integration, scaling and merging of the intensities were carried out using *MOSFLM* (Leslie, 1992) and *SCALA* from the *CCP4* suite (Collaborative Computational Project, Number 4, 1994). Molecular replacement was carried out using *AMoRe* (Navaza, 1994).

3. Results and discussion

3.1. Protein activation and purification

It has been reported that the Cry4Aa protoxin is processed into two protease-resistant fragments of 20 and 45 kDa by the intramolecular cleavage of a 65 kDa intermediate and that these two fragments need to associate to exert toxicity (Yamagiwa *et al.*, 1999). The cleavage site is after Arg235 (Angsuthanasombat *et al.*, 1993). We have recently investigated the effect of intramolecular cleavage on the toxicity of the Cry4Aa toxin by constructing a Cry4Aa single amino-acid mutant (R235Q) that is devoid of this internal cleavage site and is thus resistant to proteolysis (Boonserm *et al.*, 2004). The R235Q single mutant still retains high toxicity towards *Aedes aegypti* larvae at a level comparable to that of the wild type (Boonserm *et al.*, 2004), indicating that the mutation at this trypsin-cleavage site has no adverse effect on the Cry4Aa toxicity. The active R235Q mutant of Cry4Aa was used for the present crystallographic study. After trypsin treatment of the R235Q active mutant, a major proteolytic fragment of 65 kDa was obtained that was resistant to further proteolysis. N-terminal amino-acid sequencing after trypsin activation indicated the first residue to be Gln5, which is putatively located before helix 1 in domain I on the basis of a sequence align-

Table 1
Data-collection statistics.

Values in parentheses are for the highest resolution shell (3.05–2.95 Å).

Space group	$C222_1$
Unit-cell parameters (Å)	
a	91.20
b	202.07
c	98.73
Resolution range (Å)	20.0–2.95
Moxaicity (°)	0.5
Measured reflections	138542 (13838)
Unique reflections	19646 (1896)
Data redundancy	7.1 (7.3)
Completeness (%)	100.0 (100.0)
Average $I/\sigma(I)$	15.8 (3.7)
$R_{\rm merge}$ (%)†	13.4 (47.4)

† $R_{\rm merge} = (\sum |I_i - \langle I \rangle| / \sum I_i) \times 100$, where I_i is an individual intensity observation, $\langle I \rangle$ is the mean intensity for that reflection and the summation is over all reflections.

ment with Cry3Aa. The trypsin-activated 65 kDa fragment was purified by gel filtration for subsequent crystallization trials.

3.2. Crystallization and data collection

The 68 kDa chymotrypsin-activated Cry4Ba toxin has been crystallized previously and well ordered crystals diffracting X-rays to 1.75 Å resolution were obtained (Boonserm *et al.*, 2003). A similar approach was used in the present study to promote the crystal growth of the Cry4Aa toxin. Salts were effective precipitants and plate-shaped crystals of Cry4Aa with approximate dimensions of 0.15 × 0.15 × 0.005 mm (Fig. 1) were obtained using 0.1 *M* Tris–acetate pH 7.0 and 0.2–0.3 *M* KH_2PO_4 as precipitants.

One such crystal was used to obtain a 100% complete native data set to 2.95 Å resolution. Data-collection statistics are summarized in Table 1. Assuming the presence of one Cry4Aa molecule per asymmetric unit, the value of V_M (Matthews, 1968) is 3.60 $Å^3\,Da^{-1}$, giving a solvent content of 65%.

Figure 1
Crystals of Cry4Aa. Plate-shaped crystals (0.15 × 0.15 × 0.005 mm) can be seen in the crystallization drop.

3.3. Solution of the structure

A preliminary model of the structure was found by molecular replacement using the program *AMoRe* (Navaza, 1994). The rotation-function calculation was performed in the resolution range 20.0–4.0 Å using the Cry4Ba refined crystal structure as the search model (Li, 2004) and a Patterson integration radius of 30 Å. This model returned a weakly contrasted solution with a correlation coefficient for the structure-factor amplitudes of 0.160 (0.152 for the second highest solution) and a value of 0.27 for the intensities (0.24 for the second highest solution). This solution consistently appears as the first when varying the Patterson integration radius between 30 and 35 Å. The search model was then placed in the unit cell using the Crowther–Blow translation function with data between 9.0 and 4.0 Å resolution. This model returned a solution with a correlation coefficient of 0.157 and an *R* factor of 49.8% (0.117 and an *R* factor of 51.0% for the second highest peak). As a control, a systematic search using the Crowther–Blow translation function was carried out for the first 50 independent peaks of the rotation function in each of the space groups $C222$ and $C222_1$. This search unambiguously returned the same solution for space group $C222_1$ with the same relatively weak but significant contrast as stated above. This result is consistent with the low sequence identity between the search model Cry4Ba and Cry4Aa (35.6% for 516 aligned positions).

Rigid-body refinement yielded a correlation coefficient of 0.17 and an *R* factor of 49.6% for 7201 reflections between 9.0 and 4.0 Å resolution. Examination of the crystal packing did not reveal any steric hindrance from symmetry-related molecules. 1171 reflections randomly chosen between 20 and 2.9 Å (5% of the data) were set aside to monitor the progress of the refinement. Further refinement with each of the three protein domains treated as three independent rigid bodies followed by one cycle of molecular dynamics in torsion-angle space was carried out using *CNS* (Brünger *et al.*, 1998). This refinement returned an overall *R* factor of 34.1% for 13 814 reflections between 20 and 3.24 Å resolution and an $R_{\rm free}$ of 47.7%. Electron-density maps generated with phases from the partial model (516 residues) show several features compatible with the pattern of insertions and deletions as well as amino-acid substitutions between Cry4Aa and Cry4Ba. Refinement of the structure is now in progress using manual model building with the program *O* (Jones *et al.*, 1991) interspersed with cycles of electron-density map improvement and refinement with the programs *ARP/wARP*, *CNS* and *REFMAC* from the *CCP4* program suite (Collaborative Computational Project, Number 4, 1994). The current values for the *R* factor and $R_{\rm free}$ are 24.1 and 29.3% for all data in the resolution range 7–2.9 Å.

The authors gratefully acknowledge financial Support from the NTU *via* a startup grant, the Singapore BioMedical Research Council (to JL) and the Thailand Research Fund (to PB), as well as help and useful discussions with members of the ESRF/EMBL Joint Structural Biology Group, especially Dr Edward Mitchell.

References

Abdullah, M., Alzate, O., Mohammad, M., McNall, R. J., Adang, M. J. & Dean, D. H. (2003). *Appl. Environ. Microbiol.* 69, 5343–5353.

Angsuthanasombat, C., Crickmore, N. & Ellar, D. J. (1993). *FEMS Microbiol. Lett.* 111, 255–262.

Boonserm, P., Ellar, D. J. & Li, J. (2003). *Acta Cryst.* D59, 591–594.

Boonserm, P., Pornwiroon, W., Katzenmeier, G., Panyim, S. & Angsuthanasombat, C. (2004). *Protein Exp. Purif.* 35, 397–403.

Brünger, A. T., Adams, P. D., Clore, G. M., DeLano, W. L., Gros, P. Grosse-Kunstleve, R. W., Jiang, J.-S., Nilges, M., Pannu, N. S., Read, R. J., Rice, L. M., Simonson, T. & Warren, G. L. (1998). *Acta Cryst.* D54, 905–921.

Burton, S. L., Ellar, D. J., Jade, L. & Derbyshire, D. J. (1999). *J. Mol. Biol.* **287**, 1011–1022.

Chen, X. J., Lee, M. K. & Dean, D. H. (1993). *Proc. Natl Acad. Sci. USA*, **90**, 9041–9045.

Collaborative Computational Project, Number 4 (1994). *Acta Cryst.* **D50**, 760–763.

Crickmore, N., Zeigler, D. R., Feitelson, J., Schnepf, E., Van Rie, J., Lereclus, D., Baum, J. & Dean, D. H. (1998). *Microbiol. Mol. Biol. Rev.* 62, 807–813.

Galitsky, N., Cody, V., Wojtczak, A., Ghosh, D., Luft, J. R., Pangborn, W. & English, L. (2001). *Acta Cryst.* D57, 1101–1109.

Gazit, E., La Rocca, P., Sansom, M. S. & Shai, Y. (1998). *Proc. Natl Acad. Sci. USA*, 95, 12289–12294.

Grochulski, P., Masson, L., Borisova, S., Pusztai-carey, M., Schwartz, J. L., Brousseau, R. & Cygler, M. (1995). *J. Mol. Biol.* **254**, 447–464.

Jones, T. A., Zou, J. Y., Cowan, S. W. & Kjeldgaard, M. (1991). *Acta Cryst.*, A47, 110–120.

Jurat-Fuentes, J.-L. & Adang, M. J. (2001). *Appl. Environ. Microbiol.* 67, 323–329.

Knowles, B. H. (1994). *Adv. Insect Physiol.* **24**, 275–308.

Lee, M. K., Young, B. A. & Dean, D. H. (1995). *Biochem. Biophys. Res. Commun.* **216**, 306–312.

Leslie, A. G. W. (1992). *Int CCP4/ESF-EACBM Newsl. Protein Crystallogr.* **26**, 27–33.

Li, J. (2004). Personal communication.

Li, J., Carroll, J. & Ellar, D. J. (1991). *Nature (London)*, **353**, 815–821.

Li, J., Derbyshire, D. J., Promdonkoy, B. & Ellar, D. J. (2001). *Biochem. Soc. Trans.* **29**, 571–577.

Matthews, B. W. (1968) *J. Mol. Biol.* **197**, 375–377.

Morse, R. J., Yamamoto, T. & Stroud, R. M. (2001). *Structure*, **9**, 409–417.

Navaza, J. (1994). *Acta Cryst.* A**50**, 157–163.

Puntheeranurak, T., Uawithya, P., Potvin, L., Angsuthanasombat, C. & Schwartz, J.-L (2004). *Mol Membr. Biol.* **21**, 67–74.

Rajamohan, F., Hussain, S. R., Cotrill, J. A., Gould, F. & Dean, D. H. (1996). *J. Biol. Chem.* **271**, 25220–25226.

Roberts, L. (2002). *Science*, **298**, 82.

Schnepf, E., Crickmore, N., Van Rie, J., Lereclus, D., Baum, J., Feitelson, J., Zeigler, D. R. & Dean, D. H. (1998). *Microbiol. Mol. Biol. Rev.* **62**, 775–806.

Schwartz, J.-L., Juteau, M., Grochulski, P., Cygler, M., Prefontaine, G., Brousseau, R. & Masson, L. (1997). *FEBS Lett.* **410**, 397–402.

Smedley, P. D. & Ellar, D. J. (1996). *Microbiology*, **142**, 1617–1624.

Von Tersch, M. A., Slatin, S. L., Kulesza, C. A. & English, L. H. (1994). *Appl. Environ. Microbiol.* **60**, 3711–3717.

Walters, F. S., Slatin, S. L., Kulesza, C. A. & English, L. H. (1993). *Biochem. Biophys. Res. Commun.* **196**, 921–926.

Wolfersberger, M. G., Chen, X. J. & Dean, D. H. (1996). *Appl. Environ. Microbiol.* **62**, 279–282.

Yamagiwa, M., Esaki, M., Otake, K., Inagaki, M., Komano, T. & Sakai, H. (1999). *Appl. Environ. Microbiol.* **65**, 3464–3469.